Article

Improving selectivity, proteolytic stability, and antitumor activity of hymenochirin-1B: A novel glycosylated staple strategy

Yulei Li, Yihan Zhang, Minghao Wu, Qi Chang, Honggang Hu, and Xia Zhao

ACS Chem. Biol., **Just Accepted Manuscript** • DOI: 10.1021/acschembio.9b00046 • Publication Date (Web): 21 Feb 2019

Improving selectivity, proteolytic stability, and antitumor activity of hymenochirin-1B: A novel glycosylated staple strategy

Yulei Li[a,#], Yihan Zhang,[a,#] Minghao Wu[a], Qi Chang[a,b], Honggang Hu [c], Xia Zhao [a,b*]

[a] Key Laboratory of Marine Drugs, Ministry of Education, School of Medicine and Pharmacy, Ocean University of China, Qingdao 266003, China.

[b] Laboratory for Marine Drugs and Bioproducts, Qingdao National Laboratory for Marine Science and Technology, Qingdao 266237, China.

[c] Translational Medicine Institute, Shanghai University, Shanghai 200436, China.

*Corresponding authors:

Xia Zhao, zhaoxia@ouc.edu.cn; 1184748799@qq.com

[#] Yulei Li and Yihan Zhang contributed equally.

ABSTRACT

As host defense peptides, hymenochirin-1B has attracted increasing attention for its strong cytotoxic activities. However, its poor selectivity and proteolytic stability remain major obstacles for clinical application. To solve these problems, we designed and synthesized a series of peptide analogues of hymenochirin-1B based on cationic residue substitution and stapling combined with a glycosylation strategy. Some analogues showed improvement not only in selectivity and proteolytic stability, but also in antitumor activity. Among them, the glycosylated stapled peptide H-58 was identified as the most potential antitumor peptide. Flow cytometry and a competitive binding assay revealed that H-58 displayed significant antitumor selectivity. Confocal microscopy and nuclear staining with Hoechst dye demonstrated that H-58 entered the nucleus and caused DNA damage. In summary, the strategy of glycosylated stapled peptides is a promising approach for improving the antitumor selectivity, proteolytic stability, and antitumor activity of hymenochirin-1B, which can be used for other bioactive peptide modifications.

INTRODUCTION

Cancer is a leading cause of death worldwide and a major public health problem in developing countries.[1-2] Although great progress has been achieved in the development of cancer therapies in recent decades, most conventional chemotherapeutics exhibit insufficient selectivity, induce side effects such as neurotoxicity and so on.[3] Therefore, novel therapeutic approaches that improve cancer cell selectivity are urgently needed.

One strategy for creating novel anti-cancer agents is to take advantage of the pre-existing host innate defense mechanisms of other species.[4] Host defense peptides (HDPs) are able to discriminate between tumor and normal cells by specifically interacting with the acidic extracellular environment[5] and negatively charged membrane components, such as phosphatidylserine,[6] sialic acid,[7-8] heparan sulfate and chondroitin sulfate.[9-10] Destruction of

the target cell membrane (cytoplasm and/or mitochondria) is a major pathway of irreversible cell damage by HDPs. However, it is not the only mechanism by which cytolytic peptides can kill cancer cells. HDPs may interfere with signal transduction pathways or induce DNA damage to prevent tumors.[11] Frog skin constitutes a rich source of peptides with a wide range of biological properties,[12-13] including HDPs with cytotoxic activities against bacteria, fungi, viruses, and tumor cells.[14] The hymenochirins are a family of α-helical host-defense peptide, which first isolated from the skin secretions of the Congo clawed frog *Hymenochirus boettgeri* (pipidea). As a cationic, amphipathic, α-helical, 29-residue, host-defense peptide, hymenochirin-1B is the predominant pharmacological active component of four hymenochirins, which showed a wide of biological activities, such as antimicrobial,[15] anticancer,[16] immunomodulatory[15] and anti-diabetic activities.[17-19] However, its poor antitumor activity, proteolytic stability and selectivity remain major obstacles for clinical application.

Peptide stapling is a strategy for constraining peptides typically in a α-helical conformation and improving the proteolytic stability of peptides.[20-26] It has been applied to efficiently enhance the binding capability of many peptides with their intended targets and confer protease resistance.[27-33] In our previous study, we investigated the influence of the all-hydrocarbon stapled strategy on the biological activity and protease resistance ability of hymenochirin-1B, and found that some analogues showed improvement in protease resistance compared to the parent peptide.[34] However, the antitumor activity was not significantly improved and the selectivity was poor. Here, we designed and synthesized a series of peptide analogues of hymenochirin-1B by stepwise structural optimization. A cationic residue substitution strategy was used to improve its antitumor activity, and a stapling combined with glycosylation strategy was applied to improve its antitumor selectivity and proteolytic stability (Figure. 1).

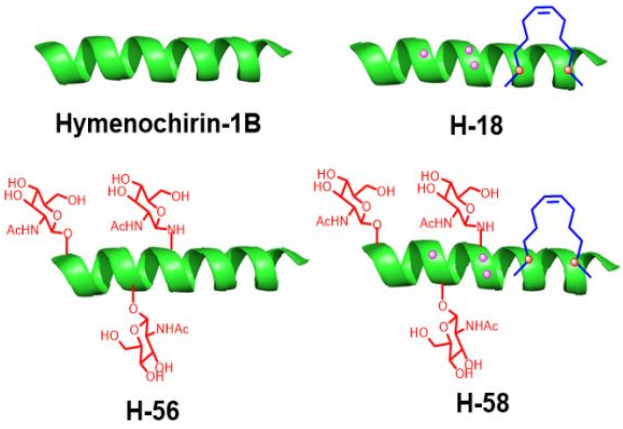

Figure 1. Structures of the linear template peptide hymenochirin-1B, stapled peptide H-18, glycosylated peptide H-56, glycosylated stapled peptide H-58. The green represents peptide chain, the blue points to the hydrophobic staple carbon chains.

RESULTS AND DISCUSSION

Stapling strategy and cationic residue substitution improved antitumor activity and proteolytic stability

In our previous all-hydrocarbon stapled strategy study, we found that an increase in positive charge may favor the electrostatic interaction of peptides with the negatively charged components of cell membranes, thus enhancing the growth-inhibitory activity against cancer cells. Therefore, we determined whether cationic amino acid substitution improved the antitumor activity of hymenochirin-1B.

Cationic residue substitution. To increase the cationicity and preserve the amphipathicity of hymenochirin- 1B, the amino acids Pro5, Glu6 and Asp9, which are on the hydrophilic face of the helix, were replaced with one or more cationic amino acids (arginine or lysine), resulting in an increased net cationic charge. All analogues showed increased potency against tumor cells compared with hymenochirin-1B (Table 1, S1). The substitution of amino acids Glu6 and Asp9 showed the similar antitumor activity and higher antitumor activity than the substitution of Pro5 in hymenochirin-1B. Among analogues, **H-14** and **H-28** which Pro5, Glu6 and Asp9 all were substituted showed potent antitumor activity and compared to other

cationic residue-substituted linear analogues. To determine whether the net charge (NC) was positively correlated with their antitumor activity. The electric neutrality residues such as serine, threonine and asparagine were substituted by lysine or arginine in hymenochirin-1B (Table S2). However, the lysine-substituted linear peptides **H-34**-**H-37** and stapled peptides **H-42**-**H-45** (NC≥12), arginine-substituted linear peptides **H-38**-**H-41** and stapled peptides **H-46**-**H-49** (NC≥12) did not exhibit stronger antitumor activity than **H-14, H-18, H-28** and **H-33** (NC<12), respectively, although they had more net charges. These results suggested that the charge was not positivity correlated with the antitumor activity of the peptides and a threshold seems to exist (6≤NC≤11).

Stapling after cationic residue substitution. Since the substitution of cationic amino acid improved the antitumor activity of hymenochirin-1B, three optimal stapling peptides **H-2**, **H-5** and **H-10** were substituted by cationic residues (arginine or lysine) to improve the antitumor activity of these stapled peptides (Table 1).[34] CD analysis demonstrated that the helicity of the lysine-substituted stapled peptides range from 49.1% to 74.0%, corresponding to a 1.1 to 1.5-fold increase over hymenochirin-1B (Table 1, Figure. 4A).

On the whole, the most stapled peptide analogues showed more potent antitumor activity and resistance to enzymatic degradation than the linear peptide analogues, which improved along with the increased net cationic charge (Table 1, S1, Figure. 4C). Among the stapled peptide analogues, the monocyclic peptide **H-18** and **H-19** showed better antitumor activity than the other analogues.

Based on the above mentioned staple and amino acid substitution strategy, **H-18** and **H-19** were selected as reference compounds for the next phase of structural modifications.

Glycosylation improve the selectivity and proteolytic stability

Although the stapling strategy and cationic amino acid substitutions improved the antitumor activity and proteolytic stability of hymenochirin-1B analogues, the high hydrophobicity conferred by the stapling significantly increased the toxicity to normal cells.[35-36] Glycosylation of peptides is a promising strategy for modulating the

physicochemical properties of peptide drugs.[37-41] To solve this problem, we designed the novel strategy glycosylating stapled peptides and determined if they decreased the hydrophobicity and improved the selectivity of peptide analogues against cancer cells.

Scanning of glycosylation position and number. The sugar linked to an asparagine residue is usually *N*-acetyl-glucosamine (GlcNAc) with always beta configuration.[42] A previous study found that the conjugation of GlcNAc to peptide decreased its lipophilicity and reduced hepatic uptake, leading to a significant increase in tumor uptake.[43] Therefore, in this study, GlcNAc was chosen as the glycosyl unit to attach to hymenochirin-1B, and the effects of glycosylation position (Asn10, Ser4, Thr7) and number were also investigated.

The synthesis of glycosylated peptides was based on the key glycoamino acid building blocks Fmoc-Asn[Ac_3GlcNAcβ]-OH, Fmoc-Thr[Ac_3GlcNAcβ]-OH and Fmoc-Ser[Ac_3GlcNAcβ]-OH (Figure. 2A-C).[44] A series of glycosylation modification peptide analogues of hymenochirin-1B were prepared by solid phase synthesis to determine the optimal glycosylation modification position and glycosylation number (Figure. 2D). CD analysis demonstrated that these peptide analogues maintained a similar helicity as hymenochirin-1B (Table S3, Figure. 4A). Interestingly, compared with the template peptide, most of the glycosylated peptide analogues showed a slightly decreased antitumor activity, which may have been due to the decreased hydrophobicity. However, H-56 (Figure. 1) maintained the same antitumor activity as the template peptide and had significantly decreased hemolytic activity (Figure S111). Therefore, we determined whether glycosylation modification could improve resistance to enzymatic degradation and maintain antitumor activity. The susceptibility of all glycosylated peptide analogues toward trypsin degradation was measured. As expected, glycosylated peptides had expected higher protease resistance than the template peptide, which was positively correlated with the number of GlcNAc modifications (Figure 4B). In addition, all three glycosylation sites on hymenochirin-1B were glycosylated. According to our previous all-hydrocarbon stapled strategy and cationic substitutions study, we found that the lysine-substituted staple peptides **H-18** and **H-19** possessed the most optimal anti- tumor activity. However, **H-18** and **H-19** were found to be increased hemolysis

on erythrocytes (Figure. S111). It may be due to high averaged hydrophobicity conferred by the stapling and increased the toxicity to normal cells. To solve this problem, we take advantage of the glycosylation strategy to decrease the hydrophobicity and improve selectivity of peptide analogues on cancer cells.

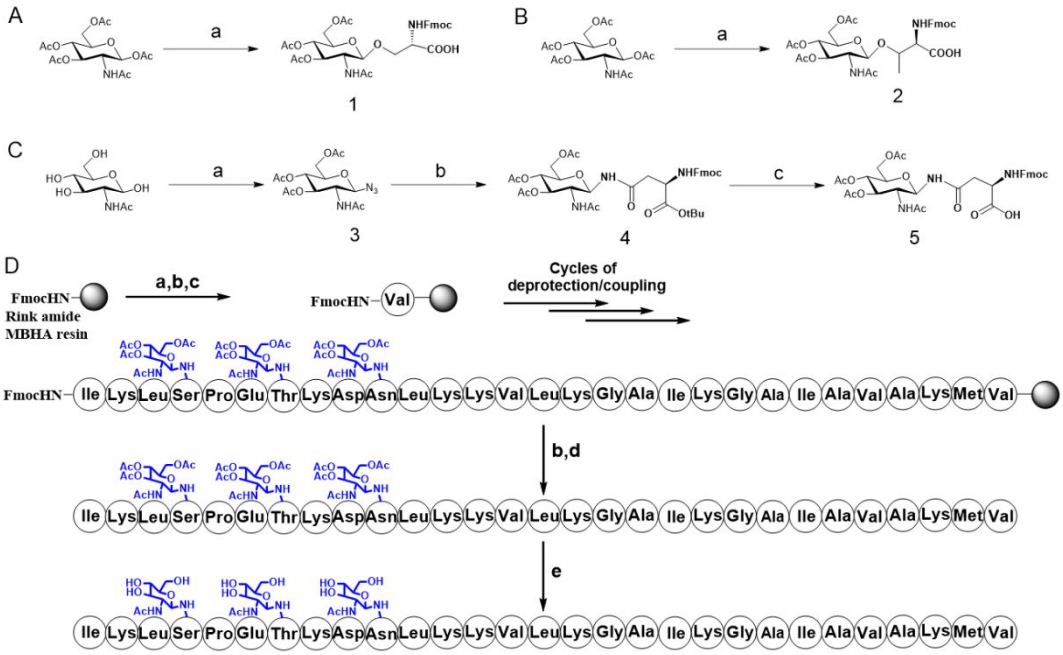

Figure 2. A) Synthetic route of building block Fmoc-Ser[Ac_3GlcNAcβ]-OH. (a) I) peracetylated GlcNAc, 4 Å molecular sieves, anhydrous DCM, $BF_3.Et_2O$, 0 ºC, overnight, II) Fmoc- serine, DCM/ MeCN (1:2), rt, 4 days, 17.0% in 2 steps; B) Synthetic route of building block Fmoc-Thr[Ac_3GlcNAcβ]-OH. (a) I) peracetylated GlcNAc, 4 Å molecular sieves, anhydrous DCM, $BF_3.Et_2O$, 0 °C, overnight, II) Fmoc-threonine, DCM/ MeCN (1:2), rt, 4 days, 38.77% in 2 steps; C) Synthetic route of building block Fmoc-Asn- [Ac_3GlcNAcβ]-OH. (a) I) acetyl chloride, rt, 4 days, II) NaN_3, tetrabutylammonium iodide, DCM/Water, rt, 1 h, 77.62% in 2 steps; (b) i) H_2, Pd/C, rt, 12 h, 2) Fmoc-Asp-OtBu, HOBt, DIC, DCM/DMF, rt, 12 h, 44.81% in 2 steps; (c) DCM/TFA (3:1, v/v), rt, 2 h, 97.4%. D) Solid-phase synthesize of stapled peptide H-56. Reagents and conditions: (a) 20% piperidine in DMF 5 min (2 times), 35 °C; (b) Fmoc-AA-OH (4equiv)/Oxyma (4equiv)/ DIC (4equiv), 20min, 60 °C; (c) Fmoc-Ser (Thr or Asn) [Ac_3GlcNAcβ]-OH (4equiv) /HATU (4equiv)/ HOAT (4equiv) / DIPEA (4equiv), 60min, 35 °C; (d) Reagent K (TFA:H_2O:EDT: thioanisole: phenol =82.5:5: 2.5: 5:5), 3 h, 35 °C. (e) sodium methoxide in the dry methanol, rt, 0.5h.

Table 1: The design, structural information and antitumor activity of modified peptides

peptide	sequence	NC	stability	IC_{50} (μM)		
			$t_{1/2}$ (h)	A549	HCT116	HepG2
H-0	I K L S P E T K D N L K K V L K G A I K G A I A V A K M V.NH_2	6	0.28	15.22±0.21	12.76±0.43	8.07±0.21
H-2	I K L S P S_5 T K D S_5 L K K V L K G A I K G A I A V A K M V.NH_2	7	0.50	4.26±0.52	3.54±0.72	1.60±0.24
H-5	I K L S P E T K D N L K K V L K G S_5 I K G S_5 I A V A K M V.NH_2	6	2.80	7.35±0.22	4.16±0.21	2.82±0.23
H-10	I K L S P S_5 T K D S_5 L K K V L K G S_5 I K G S_5 I A V A K M V.NH_2	7	3.50	3.59±0.12	3.51±0.37	1.50±0.21
H-11	I K L S P E T K K N L K K V L K G A I K G A I A V A K M V.NH_2	8	0.47	1.82±0.23	6.50±0.32	4.96±0.43
H-12	I K L S K E T K D N L K K V L K G A I K G A I A V A K M V.NH_2	7	0.42	2.35±0.31	8.09±0.40	4.28±0.38
H-13	I K L S K E T K K N L K K V L K G A I K G A I A V A K M V.NH_2	9	0.46	1.17±0.23	4.93±0.51	2.46±0.32
H-14	I K L S K K T K K N L K K V L K G A I K G A I A V A K M V.NH_2	11	0.26	0.98±0.11	1.841±0.34	4.54±0.25
H-15	I K L S K S_5 T K D S_5 L K K V L K G A I K G A I A V A K M V.NH_2	8	0.40	2.26±0.24	2.95±0.25	2.20±0.27
H-16	I K L S P S_5 T K K S_5 L K K V L K G A I K G A I A V A K M V.NH_2	9	0.42	1.85±0.31	2.65±0.35	3.14±0.46
H-17	I K L S K S_5 T K K S_5 L K K V L K G A I K G A I A V A K M V.NH_2	10	0.38	0.96±0.33	1.49±0.45	1.64±0.47
H-18	I K L S K K T K K N L K K V L K G S_5 I K G S_5 I A V A K M V.NH_2	11	0.91	0.89±0.21	1.11±0.21	1.61±0.21
H-19	I K L S K E T K K N L K K V L K G S_5 I K G S_5 I A V A K M V.NH_2	9	0.49	1.00±0.36	1.78±0.35	1.64±0.36
H-20	I K L S P S_5 T K K S_5 L K K V L K G S_5 I K G S_5 I A V A K M V.NH_2	9	3.20	2.10±0.32	2.63±0.35	4.93±0.53
H-21	I K L S K S_5 T K K S_5 L K K V L K G S_5 I K G S_5 I A V A K M V.NH_2	10	3.10	3.26±0.36	3.05±0.21	1.50±0.28
H-57	I K L S(GlcNAc) K E T K K N(GlcNAc) L K K V L K G S_5 I K G S_5 I A V A K M V.NH_2	9	1.91	1.10±0.31	1.65±0.28	2.71±0.05
H-58	I K L S(GlcNAc) K K T K K N(GlcNAc) L K K V L K G S_5 I K G S_5 I A V A K M V.NH_2	11	1.75	0.62±0.12	1.29±0.08	2.13±0.07

The red represents the conserved residues. The pink represents the lysine-substituted residues. S_5=(*S*)-N-Fmoc-2-(4'-pentenyl)alanine, NC= Net charge. Doxorubicin is a positive control.

Glycosylation decreases the hydrophobic property and improves tumor uptake. According to the investigation of glycosylation position and number on hymenochirin-1B, we found that **H-56** with three glycosylation sites (Asn10, Ser4 and Thr7) maintained similar antitumor activity as the template peptide. Therefore, the stapled peptides **H-18** and **H-19** were glycosylated respective to their three positions, and the glycosylated staple peptides **H-57** and **H-58** were obtained by solid phase synthesis, respectively (Figure 3). The retention time (RT) of reversed phase high performance liquid chromatography (RP-HPLC) typically reflects the hydrophobicity of peptides. In this study, peptides **H-18** and **H-19** displayed larger hydrophobicity (RT=17.61 and 17.53 min, respectively) (Figure S10, S11) than the glycosylated staple peptides **H-57** and **H-58** (RT=17.45 and 17.46min, respectively) (Figure S50, S51). The two glycosylated peptide analogues maintained higher proteolytic stability than the stapled peptides without glycosylation modification, and exhibited decreased hemolysis of erythrocytes and improved cell selectivity (Figure S111, 4D). **H-58** (Figure. 1) had the highest antitumor activity and cancer cell selectivity, and as such, can be regarded as an antitumor candidate.

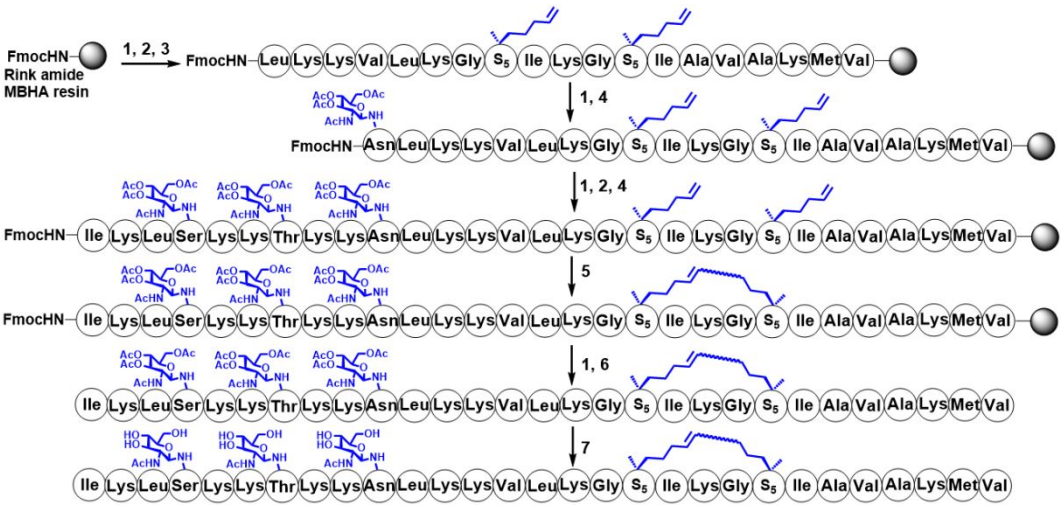

Figure 3. Solid-phase synthesize of glycosylated stapled peptide H-58. Conditions: 1) 20% piperidine in DMF 5 min (2 times), 35°C; 2) Fmoc-AA-OH (4 equiv) /Oxyma (4equiv)/ DIC (4 equiv), 20 min, 60 °C; 3) Fmoc-S_5-OH (4 equiv) /HATU (4 equiv)/ HOAT(4equiv)/DIPEA (4 equiv), 60 min, 35 °C; 4) Fmoc-Ser (Thr or Asn) [Ac_3GlcNAcβ]-OH (4equiv) /HATU (4 equiv)/ HOAT (4 equiv) / DIPEA (4 equiv), 60 min, 35 °C; 5) 6 mM 1st Grubbs, catalyst, DCE, 2 h, 35 °C; 6) Reagent K (TFA:H_2O:EDT: thioanisole: phenol =82.5:5:2.5:5:5), 3 h, 35 °C; 7) sodium methoxide in the dry methanol, rt, 0.5 h.

Protease resistance and hemolysis ability of H-58

Protease resistance. To test the protease stability of the modified peptides, we measured their susceptibility towards trypsin degradation at room temperature in phosphate-buffered saline (PBS buffer, pH 7.4), as determined by HPLC. Trypsin is a protease that predominantly cleaves at the carboxyl terminus of positively charged amino acids such as arginine and lysine. Under these conditions, the half-life ($t_{1/2}$) of hymenochirin-1B was 0.28 h. As expected, the hydrocarbon-stapled peptides and glycosylated peptides possessed higher protease resistance than the template peptide. The $t_{1/2}$ of **H-18, H-19,** and **H-56** was 0.91, 0.65, and 0.61 h, respectively. The protease resistance improved in accordance with an increase in the number of carbohydrates. Glycosylation of the stapled peptides further improved the protease stability of peptides, as the $t_{1/2}$ of **H-57** and **H-58** was 1.91 h and 1.7 h respectively (Figure 4C, S111A). These results demonstrated the superiority of glycosylated hydrocarbon-stapled peptides over linear peptides with respect to protease resistance.

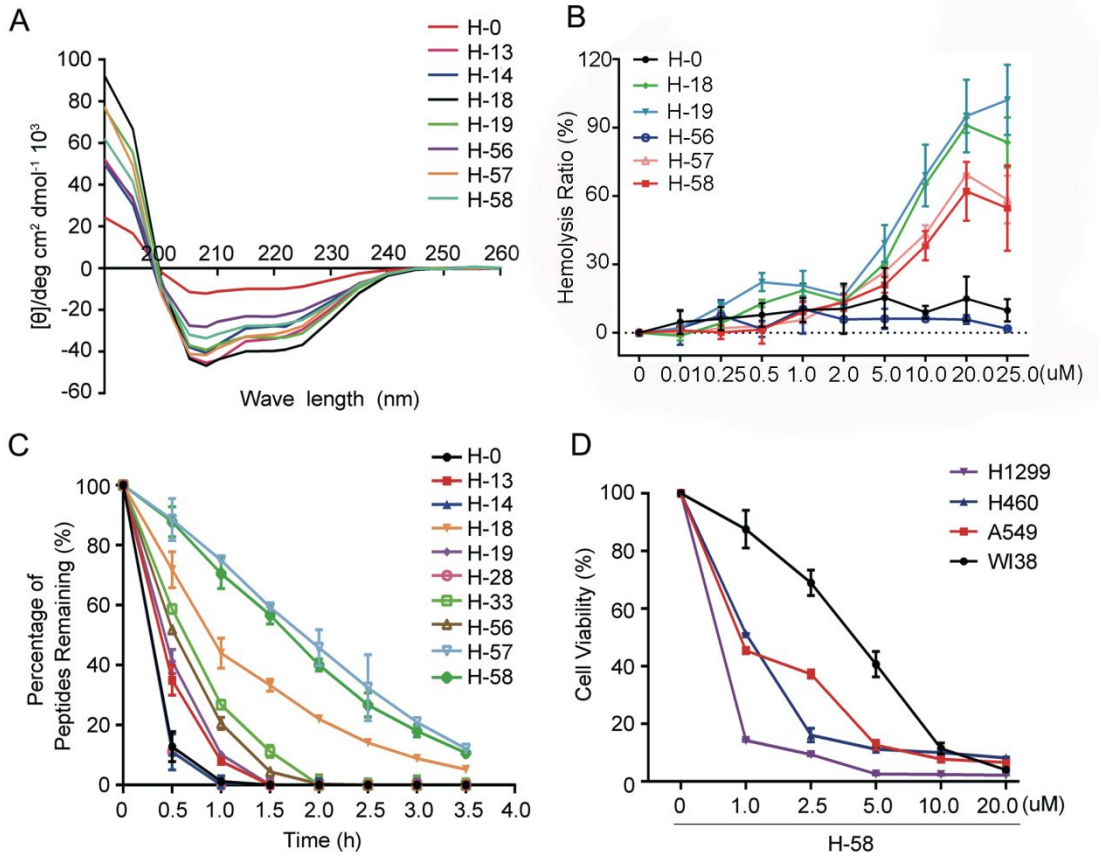

Figure 4. A) CD spectra of the stapled peptides. The peptides were dissolved in TFE and H_2O (1:1) at a final concentration of 50 mM. The percent helicity was calculated based on the $[\theta]_{222}$ value. B) Representative concentration curve of hemolysis reactions. C) Proteolytic stability of peptides incubated in trypsin solution (5 ng/μl in 50 mM PBS buffer, pH=7.4) at a final concentration of 0.1 mM. Date points are displayed as the mean value SEM of duplicate independent experiments. The percent of residual peptide was monitored by Analytic HPLC. D) Cell viability analysis of WI38, H460, NCI-H1299 and A549 cells cultured in the presence of H-58 for 48 h by MTT assay. All experiments were repeated at least three times.

Hemolytic activity. Hemolytic experiments were performed to investigate the hemolytic activity of the peptides. As shown in Figure 4B, the hemolytic rate of **H-58** was lower than

that of **H-18**, **H-19** and **H-57**, however, **H-58** had stronger anti-tumor effects than **H-0**, **H-18**, **H-19**, **H-56** and **H-57** at very low concentrations (0-1 μM, Figure S111B).

Selectivity of H-58 against cancer cells

Uptake in cancer cells. A flow cytometry assay was used to investigate **H-58** cell binding and uptake in cancer cells. **H-58** had higher binding with human non-small cell lung cancer (NCI- H1299) and human liver cancer cell (PLC) (Figure 5A-B) than **H-0**, indicating that it could reach cancer cells more efficiently than **H-0**. The tumor targeting ability of **H-58** (at 1 μM) against A549 lung cancer cell line was also studied, and the WI38 noncancerous cell line was used as a control. As shown in Figure 5C and 5D, the cellular uptake of **H-58** was much lower in WI38 cells than in A549 cells. In addition, **H-58** had high tumor targeting ability in NCI-H1299 and PLC, than in the RAW and LO-2 noncancerous cell lines (Figure 5E-F). Furthermore, the mean fluorescence intensity detected by microplate reader was also higher in cancer cells than in noncancerous cells (Figure 5G). Taken together, these data illustrated that **H-58**, a glycosylated stapled peptide, had high tumor targeting activity.

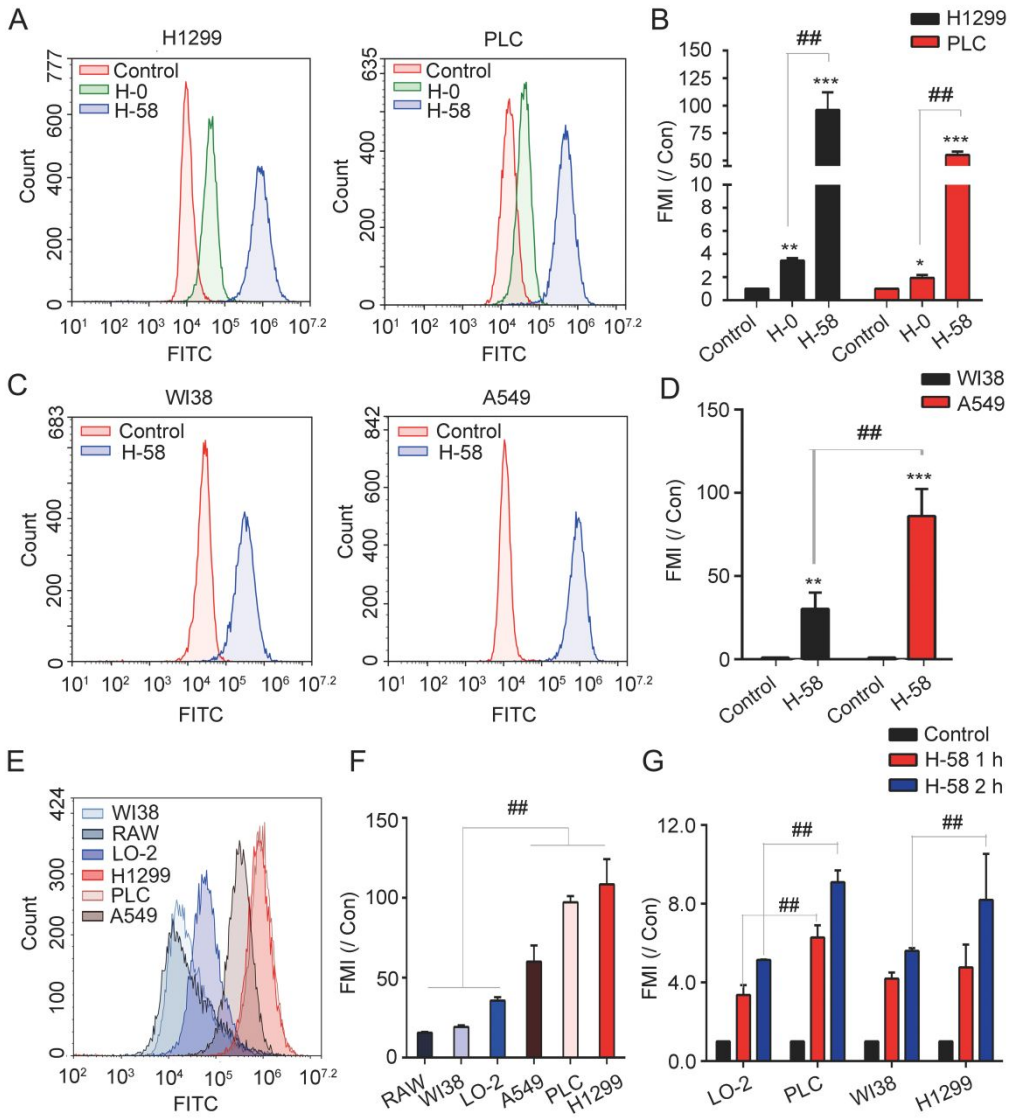

Figure 5. H-58 Had Higher Tumor Targeting Activity. A) Peptides uptake by the cancer cells NCI-H1299 and PLC was measured using ACEA NovoCyte flow cytometry. The peptides (1 μM) FITC-H-0 (green) and FITC-H-58 (blue) were incubated with the cells for 1 hour at 37 °C. B) The mean fluorescence intensity (MFI) of FITC positive cells. C) The uptake of H-58 (1 μM for 1 hour) by the noncancerous cell WI38 and cancer cell A549 was measured using ACEA NovoCyte flow cytometry. D) MFI of FITC positive cells. E) The uptake of H-58 (1 μM for 1 hour) by the noncancerous cell WI38, RAW, LO-2 and cancer cell A549, NCI-H1299 and PLC. F) MFI of FITC positive cells. G) The uptake of H-58 (1 μM for 1 h and 2 h) by the noncancerous cell WI38,

LO-2 and cancer cell H1299, PLC was measured using Microplate Reader. The data are expressed as the mean ± SD of three experiments. $^{**}p < 0.01$, $^{***}p < 0.001$ means significant difference in the same group, and $^{\#\#}p < 0.01$ means significant difference between different groups.

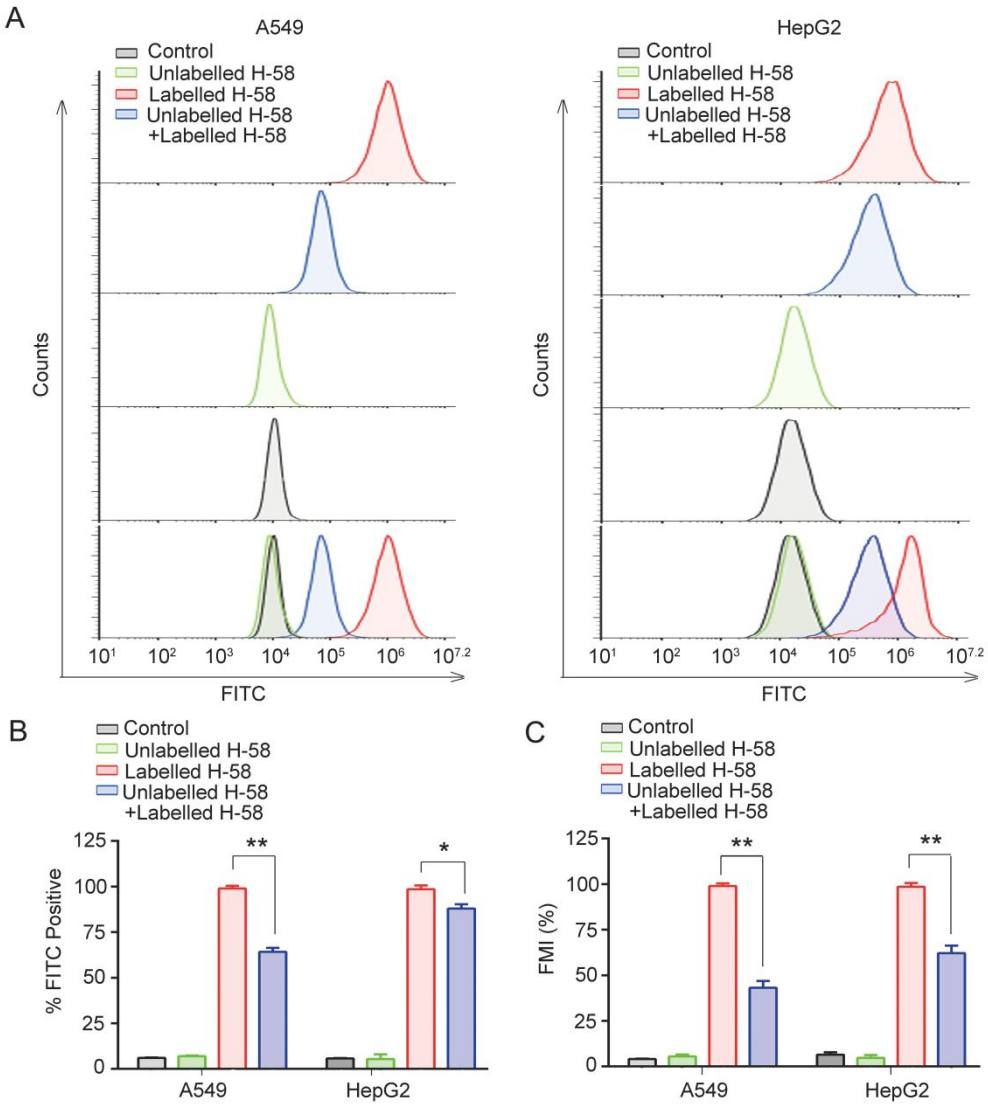

Figure 6. H-58 Had Specific Binding to Cancer Cells. A) Competitive peptides uptake by the cancer cells A549 and HepG2 were measured using ACEA NovoCyte flow cytometry. The cells were preincubated with unlabeled H-58 (5 μM) for 15 min at 37 °C. Thereafter, the FITC labeled H-58 (0.5 μM) was added and incubated for 30 min. The cells were subjected to flow cytometry, and data were analyzed using NovoExpress software. B) FITC positive cells in the absence or

presence of free H-58. C) MFI of FITC positive cells in the absence or presence of free H-58. *p < 0.05, **p < 0.01 means significant difference between absence and presence of free H-58 group.

Specific binding to cancer cells. A competitive binding assay was used to evaluate the binding specificity of **H-58** to cancer cells. The A549 and HepG2 cancer cells were pre-incubated with unlabelled **H-58** (5 μM) for 15 min at 37 °C. Then fluorescein isothiocyanate (FITC) labeled **H-58** (0.5 mM, scheme S1) was added and incubated for 30 min, after which the cells were analysed by flow cytometry. A decrease in the percentage of FITC positive occurred when the cells were incubated in the presence of excess unlabelled peptide. The percentage of FITC positive cells A549 and HepG2 cells decreased from 99% to 65%, and from 99% to 88%, respectively (Figure 6A-B); and the mean fluorescence intensity decreased from 99% to 43% and from 99% to 62% (Figure 6C), respectively. These data suggested that the specific binding of **H-58** to cancer cells and uptake of peptides were reduced when the putative receptor was occupied with excess ligand.

Next **H-58** was evaluated for binding at low temperature (4 °C). The results show that the binding of peptide was reduced compared to that observed at 37 °C (Figure S118), suggesting that once the cells are metabolically rendered inactive, the binding of peptides is severely dampened.

Apoptosis assay in cancer cells. Based on abovementioned data on the tumor targeting activity, the apoptosis assay of noncancerous and cancer cells was performed to determine if **H-58** could selectively kill cancer cells. Compared to WI38, the nuclei of cancer cells H460, NCI-H1299 and A549 were notably condensed, and a large number of nuclear fragments were observed (Figure S119 B). **H-58** promoted the apoptosis of tumor cells but had less

effect on noncancerous cells (Figure S119 A). To verify this conclusion, the median inhibitory concentration (IC_{50}) was measured using the MTT assay. As shown in Figure 4D, the IC_{50} values of **H-58** in NCI-H1299 (0.1023 μM), A549 (0.9057 μM) and H460 (0.9215 μM) were lower than those in WI38 cells (3.629 μM). These data suggested that **H-58** was more sensitive to cancer cells than noncancerous cells and exhibited higher tumor selectivity.

Mechanism of H-58 against cancer cells

Induction of cancer cell death through the apoptotic pathway. To investigate the mechanism of **H-58** in cancer cells, it was administered to HepG2 and A549 cells doses of 0.5 and 1 μM, respectively. Flow cytometry analysis of live cells showed that **H-58** induced a concentration-dependent increase (7.1-13.55% and 13.5-20.1%) in both the early and late stages of apoptosis of HepG2 and A549 cells, respectively (Figure. 7A). Caspases are a family of cysteine proteases that function as key mediators of programmed cell death or apoptosis, and caspase-3 is activated during the early stages of apoptosis.[45] In this study, Western blot analyses showed that H-58 promoted the activation of caspase-3 (Figure 7B). To investigate the anti-proliferative efficacy of **H-58**, we performed a colony formation assay. As shown in Figure 8C, fewer and smaller colonies were formed in HepG2 and A549 cells treated with **H-58** compared to the control cells. These results indicated that **H-58** significantly induced cell apoptosis and inhibited tumor cell growth.

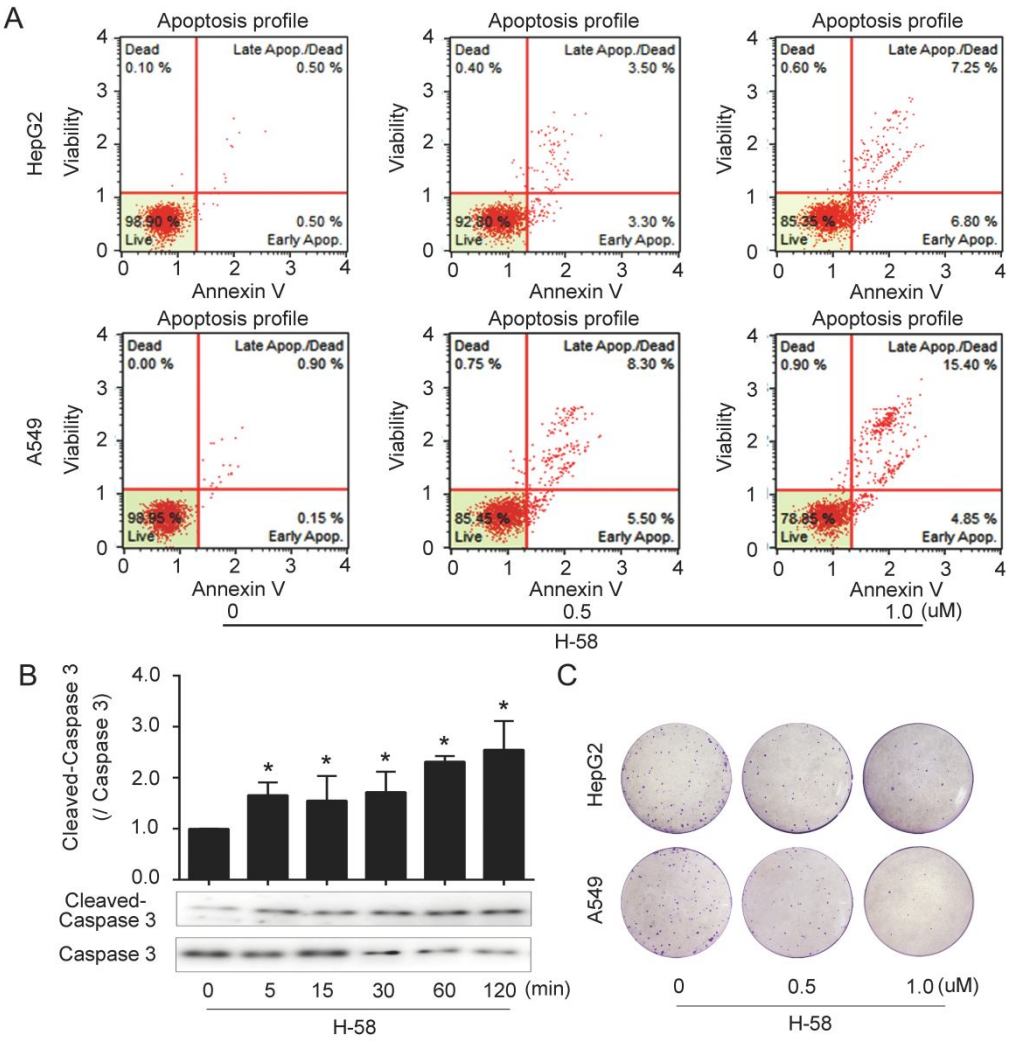

Figure 7. H-58 Induces Cancer Cell Death Through Apoptotic Pathway. A) Flow cytometric assay of HepG2 and A549 cells after 2 h of incubation with the indicated concentrations (0.5, 1 μM) of H-58. B) Induction of Cleavage of Caspase-3 in A549 Cells treated with H-58 (1 μM) was probed by western blotting. C) Colony formation of A549 cells HepG2 and A549 cells treated with H-58. The data are expressed as the mean ± SD of three experiments. *$p < 0.05$ means significant difference between control and H-58 groups.

H-58 increase DNA damage in cells. To further explore how **H-58** promoted the apoptosis of cancer cells, FITC-labelled peptides were synthesized to analyse their location in cancer cells (scheme S1). FITC-β-Ala-H-0 (hymenochirin-1B), and **H-58** efficiently entered the

cytoplasm of A549 cells after 1 h (Figure S120), while nearly no fluorescence was found in non-drug treated control cells. Interestingly, some green fluorescence of FITC-β-Ala-**H-58** was detected in the nucleus, but the green fluorescence of FITC-β-Ala-H-0 was not detected even after extending the incubation period. These results suggested that the glycosylated stapled peptide **H-58** may have entered into the cell nucleus to against cancer cell.

Nucleus staining with Hoechst dye was performed to directly observe changes in the nuclei of apoptotic cells induced by **H-58**. As shown in Figure. S112, the nuclei were notably condensed, and a large number of nuclear fragments were observed compared with the absence of peptide, indicating that **H-58** induced cancer cell death by damaging DNA.

CONCLUSIONS

In this study, we successfully improved the antitumor selectivity and proteolytic stability of hymenochirin-1B by using a novel strategy of glycosylation combined with stapling. By applying the stapling and cation substituting strategies, we obtained the improved antitumor activity peptides **H-18** and **H-19**. By using a glycosylation strategy on stapled peptide for the first time, we obtained the optimal peptide **H-58** with high antitumor selectivity and proteolytic stability. The results of clonogenic assay, caspase-3 detection, subcellular localization, cell uptake, competitive binding assay and Hoechst nuclei staining suggest that **H-58** induces cancer cell apoptosis by DNA lesion. Further studies are needed to determine the specific binding site and antitumor mechanism of **H-58**. The strategy of glycosylation staple peptide may also be beneficial for improving the antitumor selectivity and proteolytic

stability of other bioactive peptides.

METHODS

Peptides synthesis

All peptides were synthesized via the Fmoc solid-phase peptide synthesize method using Rink Amide MBHA resin. Oxyma [ethyl 2-cyano-2-(hydroxyimino) acetate] was used as the coupling reagent, which is more effective and has a lower rate of racemization than other coupling reagents.[34] After linear peptide assembly was completed, the olefin-containing peptide was stapled using Grubbs' first-generation catalyst. The peptide was cleaved from the resin and globally deprotected with reagent K (TFA: H_2O: EDT: thioanisole: phenol =82.5: 5: 2.5: 5: 5). Pre-cooled diethyl ether was added to the crude peptide precipitates, and the peptides were purified by reversed-phase HPLC system and analyzed to confirm ≥95% purity (Figure. 2, 3).

Solid-phase peptide synthesis (SPPS):

Chain elongation: Rink Amide MBHA resin (350 mg, 0.35 mmol/g loading capacity) was swollen with dichloromethane (DCM, 5 mL) for 1 h in a fritted syringe. After removing the DCM, 20% v/v piperidine in dimethylformamide (DMF, 5 mL) was added to the beads in the syringe and allowed to shake on a tabletop shaker for 20 min twice at 37 °C. Following this, the resin was washed with DMF (3×, 5 mL), DCM (3×, 5 mL), DMF (3×, 5 mL), respectively. In a small glass vial, Fmoc-AA-OH (1 mmol), Oxyma (1 mmol), Diisopropylcarbodiimide (DIC,1 mmol) and N-Methyl pyrrolidone (NMP, 6 mL) were mixed and allowed to stand for 15 minutes at room temperature. The contents of the vial were then applied to the resin beads

and allowed to shake for approximately 30min at 60 °C. The resin was then sequentially washed thoroughly with DMF (3×, 5.00 mL), DCM (3×, 5.00 mL), DMF (3×, 5.00 mL), respectively, and then the resin was dried under a stream of air. For couplings of S_5 and glycoamino acids, Fmoc-(S_5)-OH or glycoamino acid (1 mmol), HATU (1 mmol), HOAT (1 mmol) , DIPEA (1 mmol) and DMF (6 mL) were mixed for 1 min and then added to the resin at room temperature. After 1 hour, the resin was sequentially washed with DMF (3×, 5 mL), DCM (3×, 5 mL), and DMF (3×, 5 mL). The deprotection, coupling and washing steps were repeated until all the amino acid residues were sequentially installed to construct the glycosylation stapled peptide.

Stapling of the peptide: The ring-closing metathesis reaction was carried out in 1,2-dichloroethane (DCE) at 35 °C using Grubbs' first-generation catalyst. The resin was washed with DCM (3×, 5 mL) and DCE (3×, 5 mL), and then treated with 10 mM solution of Grubbs' first-generation catalyst in DCE. After the first round of 2 h metathesis, the same procedure was repeated for a second round of catalyst treatment with fresh catalyst solution, then the peptide-resin was washed with DMF (3×, 5 mL), DCM (3×, 5 mL).

Peptide cleavage from the resin and isolation: The peptide-bound resin was treated with 20% piperidine/DMF to remove the Fmoc group from the N-terminus, and the resin was dried under a stream of air. The beads were transferred to a small glass vial and brought up in the following cocktail: 5.0% v/v deionized water (0.75 mL), 2.5% v/v ethanedithiol (EDT, 0.375 mL), 5.0 % v/v thioanisole (0.75 mL), 5.0% v/v phenol (0.75 mL) in 82.5% v/v trifluoroacetic acid (TFA, 12.375 mL). The resultant solution was allowed to shake for ~3 h at room temperature. When completed, the cocktail was applied across the syringe frit, allowing the

beads to be collected and discarded. The flow-through cocktail was collected in a polypropylene tube (~15.00 mL), and TFA was evaporated by blowing with Argon. The crude peptides were obtained by precipitation with 35 mL of cold diethyl ether and centrifugation at 3500 r/min for 3 min (3 times). The supernatant diethyl ether was decanted and the crude peptides were allowed to air dry.

***Deprotection of acetyl group protocol*:** The crude peptide was dissolved in dry methanol, and then sodium methoxide (5.4M) was slowly added into the reaction mixture and the concentration of sodium methoxide was diluted to 5.4 mM. Then the reaction mixture was stirred at room temperature for 0.5 h. The reaction process was monitored by RP-HPLC and the reaction mixture was neutralized by acetic acid.

***Fluorescent labelling of peptides protocol*:** After elongation of peptide starting from Rink amide resin (0.35 mmoL/g), the metathesis reaction was carried out for 4 h following the general protocol. Then, the Fmoc group was removed and the resin was treated with Fmoc-β-Ala (2 equiv.), HCTU (2 equiv.) as coupling reagent and DIEA (4 equiv.) for 1 h at room temperature. Fmoc group was removed and resin was treated with fluorescein isothiocyanate (FITC, 2 equiv.) and DIPEA (3 equiv.) at room temperature overnight. The cleavage was carried out following the general protocol and the crude was purified by reverse phase chromatography using semi-preparative HPLC to give the final product.

***Purification of peptides by RP-HPLC*:** The target compounds were purified by the SHIMADZU (LC-6A) RP-HPLC. The purification was carried out using a C_{18} column (Daisogel, 20×250 mm) at a flow rate of 10 mL/min. Buffer A consisted of acetonitrile with 0.1% TFA, while buffer B contained water with 0.1% TFA. The target compounds were

purified by eluting with up to 75% buffer A in 50 min in a linear gradient, starting from 10% buffer A.

ASSOCIATED CONTENT

Supporting Information

The Supporting Information is available free of charge on the ACS Publications website at DOI: xxx

Full details of experimental procedures, HPLC data to establish final product purity and HR-MS data to establish final product molecular weight.^{1}H NMR, ^{13}C NMR and ESI-MS spectra of the three glycoamino acid intermediates; hemolytic activity curves of the peptides; the figure of hoechst nuclei staining.

AUTHOR INFORMATION

Corresponding Author

*E-mail: zhaoxia@ouc.edu.cn

Address: School of Medicine and Pharmacy, Ocean University of China, Qingdao 266003, P. R. China.

Author Contributions

#Yulei Li. and Yihan Zhang contributed equally. Yulei Li designed and synthesized all compounds. Yihan Zhang conducted antitumor activity and mechanism assays in vitro. Minghao Wu , Qi Chang, Hong-gang Hu assessed the results. Xia Zhao designed this experiments, supervised the research work and revised the paper.

Notes

The authors declare no competing financial interest.

ACKNOWLEDGMENTS

This research was supported by NSFC-Shandong Joint Fund (U1606403) and Innovation Project of Qingdao National Laboratory for Marine Science and Technology (No.2015ASKJ02). We are grateful to the Instrumental Analysis Center of Ocean University of China for NMR spectroscopic and mass spectrometric analysis.

ABBREVIATIONS USED

HDPs, Host defense peptides; PS, phosphatidylserine; HOBt, 1-hydroxybenzotriazole; DIC, N,N-diisopropylc arbodiimide; TFE, trifluoroethyl; CD, circular dichroism; SPPS, solid-phase peptide synthesis; HATU, O-(7-azaben zotriazol-1-yl)-N,N,N',N'-tetrame- thylur oniumhexafluoro-phosphate; HOAT, 1-hydroxy-7-azabenzotriazole; EDT, ethanedithiol; TFA, trifluoroacetic acid; R, arginine; K, lysine; DCM, dichloromethane; DMF, N, N-dimethylformamide; GlcNAc, N-acetyl-glucosamine; RT, retention time.

REFERENCES

(1) Siegel, R. L.; Miller, K. D.; Jemal, A. (2016) Cancer statistics. *CA Cancer J Clin*. 66, 7-30.

(2) Riedl, S.; Zweytick, D.; Lohner, K. (2011) Membrane-active host defense peptides--challenges and perspectives for the development of novel anticancer drugs. *Chem Phys Lipids*. 164, 766-81.

(3) Cassidy, J.; Misset, J. L. (2002) Oxaliplatin-related side effects: characteristics and management. *Semin Oncol*. 29, 11-20.

(4) Hoskin, D. W.; Ramamoorthy, A. (2008) Studies on anticancer activities of antimicrobial peptides. *Biochim Biophys Acta*. 1778, 357-75.

(5) Makovitzki, A.; Fink, A. Shai, Y. (2009) Suppression of human solid tumor growth in mice by intratumor and systemic inoculation of histidine-rich and pH-dependent host defense-like lytic peptides. *Cancer Res.* 69, 3458-63.

(6) Bevers, E. M.; Comfurius, P.; Zwaal, R. F. (1996) Regulatory mechanisms in maintenance and modulation of transmembrane lipid asymmetry: pathophysiological implications. *Lupus.* 5, 480-7.

(7) Wang, F. L.; Cui, S. X.; Sun, L. P.; Qu, X. J.; Xie, Y. Y.; Zhou, L.; Mu, Y. L.; Tang, W.; Wang, Y. S. (2009) High expression of alpha 2, 3-linked sialic acid residues is associated with the metastatic potential of human gastric cancer. *Cancer Detect Prev.* 32, 437-43.

(8) Cazet, A.; Julien, S.; Bobowski, M.; Krzewinski-Recchi, M. A.; Harduin-Lepers, A. (2010) Groux-Degroote, S.; Delannoy, P. Consequences of the expression of sialylated antigens in breast cancer. *Carbohydr Res.* 345, 1377-83.

(9) Sugahara, K. (2003) Recent advances in the structural biology of chondroitin sulfate and dermatan sulfate. *Current Opinion in Structural Biology.* 13, 612-620.

(10) Tkachenko, E.; Rhodes, J. M.; Simons, M. (2005) Syndecans: new kids on the signaling block. *Circ Res.* 96, 488-500.

(11) Papo, N., and Shai, Y. (2005) Host defense peptides as new weapons in cancer treatment, *Cell Mol Life Sci* 62, 784-790.

(12) Ohsaki Y, Gazdar AF, Chen HC, Johnson BE. (1992) Antitumor activity of magainin analogues against human lung cancer cell lines. *Cancer Research*. 52, 3534-3538.

(13) Mechkarska, M.; Prajeep, M.; Coquet, L.; Leprince, J.; Jouenne, T.; Vaudry, H.; King, J. D.; Conlon, J. M. (2012) The hymenochirins: a family of host-defense peptides from the Congo dwarf clawed frog Hymenochirus boettgeri (Pipidae). *Peptides.* 35, 269-75.

(14) Conlon, J. M.; Mechkarska, M.; Lukic, M. L.; Flatt, P. R. (2014) Potential therapeutic applications of multifunctional host-defense peptides from frog skin as anti-cancer, anti-viral, immunomodulatory, and anti-diabetic agents. *Peptides.* 57, 67-77.

(15) Mechkarska, M.; Prajeep, M.; Radosavljevic, G. D.; Jovanovic, I. P.; Al Baloushi, A.; Sonnevend, A.; Lukic, M. L.; Conlon, J. M. (2013) An analog of the host-defense peptide hymenochirin-1B with potent broad-spectrum activity against multidrug-resistant bacteria and immunomodulatory properties. *Peptides.* 50, 153-9.

(16) Attoub, S.; Arafat, H.; Mechkarska, M.; Conlon, J. M. (2013) Anti-tumor activities of the host-defense peptide hymenochirin-1B. *Regul Pept.* 187, 51-6.

(17) Papo, N.; Seger, D.; Makovitzki, A.; Kalchenko, V.; Eshhar, Z.; Degani, H.; Shai, Y. (2006) Inhibition of tumor growth and elimination of multiple metastases in human prostate and breast xenografts by systemic inoculation of a host defense-like lytic peptide. *Cancer Res.* 66, 5371-8.

(18) Mader J S.; Hoskin D W. (2006) Cationic antimicrobial peptides as novel cytotoxic agents for cancer treatment. *Expert Opinion on Investigational Drugs.* 15, 933-946.

(19) Schweizer, F. Cationic amphiphilic peptides with cancer-selective toxicity. *Eur J Pharmacol* **2009,** 625, 190-4.

(20) Lau, Y. H.; de Andrade, P.; Wu, Y.; Spring, D. R. (2015) Peptide stapling techniques based on different macrocyclisation chemistries. *Chem Soc Rev.* 44, 91-102.

(21) Schafmeister C E, Julia Po A, Verdine G L. (2000) An All-Hydrocarbon Cross-Linking System for Enhancing the Helicity and Metabolic Stability of Peptides. *J. Am.Chem.Sco*.122, 5891-5892.

(22) Walensky, L. D.; Kung, A. L.; Escher, I.; Malia, T. J.; Barbuto, S.; Wright, R. D.; Wagner, G.; Verdine, G. L.; Korsmeyer, S. J. (2004) Activation of apoptosis in vivo by a hydrocarbon-stapled BH3 helix. *Science.* 305, 1466-70.

(23) Chang, Y. S.; Graves, B.; Guerlavais, V.; Tovar, C.; Packman, K.; To, K. H.; Olson, K. A.; Kesavan, K.; Gangurde, P.; Mukherjee, A.; Baker, T.; Darlak, K.; Elkin, C.; Filipovic, Z.; Qureshi, F. Z.; Cai, H.; Berry, P.; Feyfant, E.; Shi, X. E.; Horstick, J.; Annis, D. A.; Manning, A. M.; Fotouhi, N.; Nash, H.; Vassilev, L. T.; Sawyer, T. K. (2013) Stapled alpha-helical peptide drug development: a potent dual inhibitor of MDM2 and MDMX for p53-dependent cancer therapy. *Proc Natl Acad Sci U S A.*110, E3445-54.

(24) Walensky, L. D.; Bird, G. H. (2014) Hydrocarbon-stapled peptides: principles, practice, and progress. *J Med Chem.* 57, 6275-88.

(25) Shepherd N E, Hoang H N, Abbenante G, David P. Fairlie. (2005) Single turn peptide alpha helices with exceptional stability in water *J. Am.Chem.Sco.* 127, 2974-83.

(26) Harrison, R. S.; Shepherd, N. E.; Hoang, H. N.; Ruiz-Gomez, G.; Hill, T. A.; Driver, R. W.; Desai, V. S.; Young, P. R.; Abbenante, G.; Fairlie, D. P. (2010) Downsizing human, bacterial, and viral proteins to short water-stable alpha helices that maintain biological potency. *Proc Natl Acad Sci U S A.* 107, 11686-91.

(27) Griffiths J R. (1991) Are cancer cells acidic?. *British Journal of Cancer* . 64, 425-427.

(28) Moellering, R. E.; Cornejo, M.; Davis, T. N.; Del Bianco, C.; Aster, J. C.; Blacklow, S.

C.; Kung, A. L.; Gilliland, D. G.; Verdine, G. L.; Bradner, J. E. (2009) Direct inhibition of the NOTCH transcription factor complex. *Nature.* 462, 182-8.

(29)Sawyer, T. K.; Partridge, A. W.; Kaan, H. Y. K.; Juang, Y. C.; Lim, S.; Johannes, C.; Yuen, T. Y.; Verma, C.; Kannan, S.; Aronica, P.; Tan, Y. S.; Sherborne, B.; Ha, S.; Hochman, J.; Chen, S.; Surdi, L.; Peier, A.; Sauvagnat, B.; Dandliker, P. J.; Brown, C. J.; Ng, S.; Ferrer, F.; Lane, D. P. (2018) Macrocyclic alpha helical peptide therapeutic modality: A perspective of learnings and challenges. *Bioorg Med Chem.* 26, 2807-2815.

(30) A, D. d. A.; Lim, J.; Wu, K. C.; Xiang, Y.; Good, A. C.; Skerlj, R.; Fairlie, D. P. (2018) Bicyclic Helical Peptides as Dual Inhibitors Selective for Bcl2A1 and Mcl-1 Proteins. *J Med Chem.* 61, 2962-2972.

(31) Quach, K.; LaRochelle, J.; Li, X. H.; Rhoades, E.; Schepartz, A. (2018) Unique arginine array improves cytosolic localization of hydrocarbon-stapled peptides. *Bioorg Med Chem.* 26, 1197-1202.

(32) Iegre, J.; Ahmed, N. S.; Gaynord, J. S.; Wu, Y.; Herlihy, K. M.; Tan, Y. S.; Lopes-Pires, M. E.; Jha, R.; Lau, Y. H.; Sore, H. F.; Verma, C.; DH, O. D.; Pugh, N.; Spring, D. R. (2018) Stapled peptides as a new technology to investigate protein-protein interactions in human platelets. *Chem Sci.* 9, 4638-4643.

(33) Wu, Y.; Li, Y. H.; Li, X.; Zou, Y.; Liao, H. L.; Liu, L.; Chen, Y. G.; Bierer, D.; Hu, H. G. (2017) A novel peptide stapling strategy enables the retention of ring-closing amino acid side chains for the Wnt/beta-catenin signalling pathway. *Chem Sci.* 8, 7368-7373.

(34) Li, Y.; Wu, M.; Chang, Q.; Zhao, X. (2018) Stapling strategy enables improvement of antitumor activity and proteolytic stability of host-defense peptide hymenochirin-1B. *RSC*

Advances. 8, 22268-22275.

(35) Stone, T. A.; Cole, G. B.; Nguyen, H. Q.; Sharpe, S.; Deber, C. M. (2018) Influence of hydrocarbon-stapling on membrane interactions of synthetic antimicrobial peptides. *Bioorg Med Chem.*26, 1189-1196.

(36) Glukhov, E.; Burrows, L. L.; Deber, C. M. (2008) Membrane interactions of designed cationic antimicrobial peptides: the two thresholds. *Biopolymers.*89, 360-71.

(37) Moradi, S. V.; Hussein, W. M.; Varamini, P.; Simerska, P.; Toth, I. (2016) Glycosylation, an effective synthetic strategy to improve the bioavailability of therapeutic peptides. *Chem Sci.* 7, 2492-2500.

(38) Sola, R. J.; Al-Azzam, W.; Griebenow, K. (2006) Engineering of protein thermodynamic, kinetic, and colloidal stability: Chemical Glycosylation with monofunctionally activated glycans. *Biotechnol Bioeng.* 94, 1072-9.

(39) Sola, R. J.; Griebenow, K. (2009) Effects of glycosylation on the stability of protein pharmaceuticals. *J Pharm Sci.* 98, 1223-45.

(40) Banks, D. D. (2011) The effect of glycosylation on the folding kinetics of erythropoietin. *J Mol Biol.* 412, 536-50.

(41)Calvaresi, E. C.; Hergenrother, P. J. (2013) Glucose conjugation for the specific targeting and treatment of cancer. *Chem Sci.* 4, 2319-2333.

(42) Hu H , Xue J , Swarts B M . (2009) Synthesis and antibacterial activities of N-glycosylated derivatives of tyrocidine A, a macrocyclic peptide antibiotic. J. Med. Che. 52, 2052-2059.

(43) Haubner R.; Wester H J.; Burkhart F.; Senekowitsch-Schmidtke R.; Weber W.;

Goodman SL.; Kessler H.; Schwaiger M. (2001) Glycosylated RGD-containing peptides: tracer for tumor targeting and angiogenesis imaging with improved biokinetics *J Nucl Med.* 42,326-336.

(44) Arsequell, G.; Krippner, L.; Dwek, R. A.; & Wong, S. Y. C. (1994) Building blocks for solid-phase glycopeptide synthesis: 2-acetamido-2-deoxy-β-d-glycosides of fmocseroh and fmocthroh. *J Am Chem Soc*. 20, 2383-2384.

(45) Kobayashi, T.; Masumoto, J.; Tada, T.; Nomiyama, T.; Hongo, K.; Nakayama, J. (2007) Prognostic significance of the immunohistochemical staining of cleaved caspase-3, an activated form of caspase-3, in gliomas. *Clin Cancer Res.* 13, 3868-74.

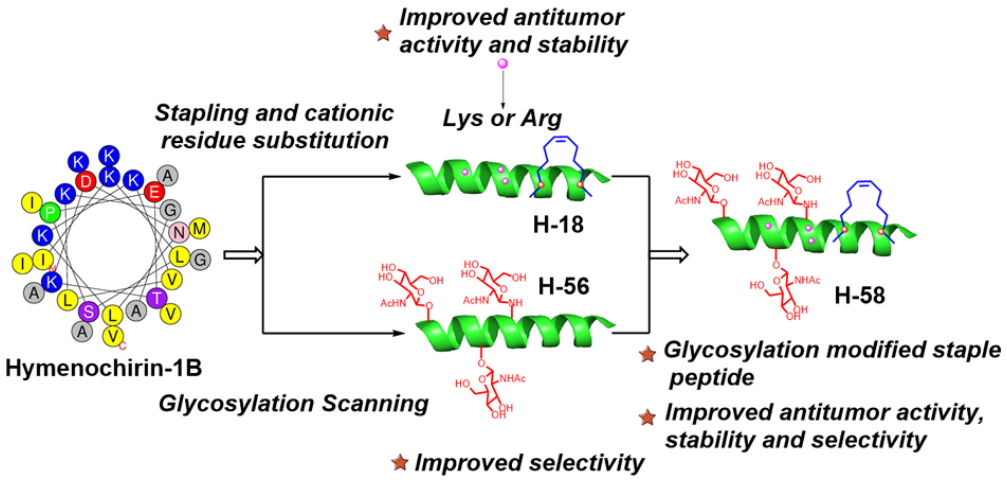

A novel glycosylated staple strategy was successfully developed and used to improve the antitumor activity, stability and selectivity of host-defense peptide Hymenochirin-1B.

80x38mm (300 x 300 DPI)